

# Single-Cycle Gap Soliton in a Subwavelength Structure

Xiao-Tao Xie\* and Mihai A. Macovei†

Max-Planck-Institut für Kernphysik, Saupfercheckweg 1, D-69117 Heidelberg, Germany

(Dated: November 20, 2018)

We demonstrate that a single sub-cycle optical pulse can be generated when a pulse with a few optical cycles penetrates through resonant two-level dense media with a subwavelength structure. The single-cycle gap soliton phenomenon in the full Maxwell-Bloch equations without the frame of slowly varying envelope and rotating wave approximations is observed. Our study shows that the subwavelength structure can be used to suppress the frequency shift caused by intrapulse four-wave mixing in continuous media and supports the formation of single-cycle gap solitons even in the case when the structure period breaks the Bragg condition. This suggests a way toward shortening high-intensity laser fields to few- and even single-cycle pulse durations.

PACS numbers: 42.65.Re, 42.65.Tg, 42.50.Gy

The recent development of ultrafast science technology allowed the generation of light pulses with durations down to few optical cycles. There is an increasing number of investigations and experiments which involve such ultrashort pulses in femtosecond and attosecond domains [1]. Applications also include control of chemical reactions in physicochemical processes [2], femtochemistry [3], biological multiphoton imaging [4] and coherent control schemes [5]. In order to study light-matter interaction under extreme conditions as the pulse approaches the duration of a single optical cycle, great efforts for the generation of still shorter pulses have been made [6–8]. In particular, for continuous media the concept of single-cycle nonlinear optics [9] as well as the notion of extreme nonlinear optics [10] were introduced. For these processes, the traditional frame of the slowly varying envelope approximation (SVEA) and the rotating wave approximation (RWA) is invalid [11].

In the last decade, there has been a rapid progress in the field of materials with periodic structures, such as Bragg grating, photonic band gap crystals and waveguide arrays [12]. Such systems exhibit qualitatively novel and fascinating linear-optical, nonlinear-optical and quantum-optical properties which provides an attractive way to control the light propagation and light-matter interaction. Nonlinear pulse propagation in periodic structures is of both fundamental and applied interest, particularly, as a potential basis for nonlinear filtering, switching and distributed-feedback amplification [13]. Few-cycle pulse propagation in continuous media can yield solitons. Solitons can also exist in periodic structures which is usually referred to as gap soliton since they only exist within the forbidden gap [14, 15]. The gap soliton was primarily found in periodic Kerr-nonlinear media. An essentially different mechanism of gap soliton generation with self-induced transparency has been revealed in Bragg grating which consists of a periodic array of thin layers of a resonant two-level medium separated by half-wavelength nonabsorbing dielectric layers [16, 17]. It should be pointed out that for such a struc-

ture, the thickness of each two-level medium layer is much smaller than the wavelength of the electromagnetic wave which propagates. Optical soliton propagation results from an interplay between dispersion and the nonlinear response of the medium which balance the nonlinear and linear effects [18]. Optical temporal solitons have become a promising candidate for optical communication networks. Thus, it is an important issue whether or not optical solitons can exist under extreme conditions, such as pulses with few optical cycles or less formed in a periodic structure. The ability to reduce the cycle number in these systems would be of particular significance.

Therefore, in this Letter we present theoretical evidence of a sub-cycle gap soliton. An extremely short pulse propagating through a one-dimensional periodic structure that consists of periodic thin layers containing resonant two-level atoms separated by a transparent material is considered (see Fig. 1). We assumed that the extremely short pulse propagates along the  $\xi$  axis to an input interface of the periodic structure at  $\xi = 0$  (a set of dimensionless time and space coordinates were taken, namely  $T = t\omega_0$  and  $\xi = z/\lambda_0$  with the carrier frequency  $\omega_0$  and wavelength  $\lambda_0$ ). First, the incident pulse moves in the free space and then partially penetrates into the subwavelength structure. In the following, the penetrating part passes through and exits into the free space. The length of the structure is  $L$ . We found that at resonance

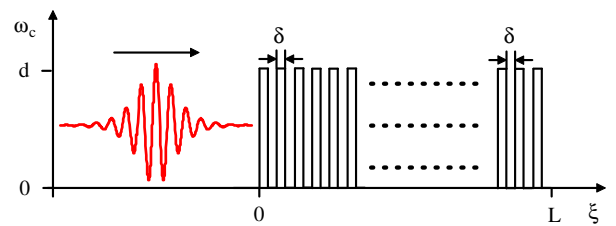


FIG. 1: (color online) Spatial distribution of atomic medium. The red curve illustrates the incident wave with few optical cycles. Symbol "→" denotes the propagation direction axis.

and for a periodic structure satisfying the Bragg condition for moderate densities, the penetrating and reflected pulse spectrum is located around the transition frequency which is distinct from the results of few-cycle propagation in a continuous media. There, a large frequency shift of the transmitted and reflected pulses was reported [8]. For particular parameters, we obtain a gap soliton with less than one optical cycle even when the structure period does not fulfill the Bragg condition. Thus, the system we propose allows the observation of different tendencies in the spectral and temporal evolution of ultrashort pulses leading to interesting and practically significant regimes of ultrashort-pulse quantum dynamics. Finally, these periodic structures can be realized by using a periodic doped fiber waveguide [15] or quantum wells embedded in a semiconductor structure [19].

In order to investigate the electromagnetic field propagation in the periodic structure, we adopt the full Maxwell-Bloch equations solved by a finite difference time-domain method [20] which has been proved to be an accurate tool. In this case, the evolution of the few-cycle electromagnetic field amplitudes  $E_x(T, \xi)$  and  $H_y(T, \xi)$ , the complex atomic polarization  $\frac{1}{2}u(T, \xi) + \frac{i}{2}v(T, \xi)$ , and the inversion population  $w(T, \xi)$  obey the following set of Maxwell-Bloch equations:

$$\begin{aligned} \frac{\partial}{\partial T} H &= -\frac{1}{2\pi} \frac{\partial}{\partial \xi} E, \\ \frac{\partial}{\partial T} E &= -\frac{1}{2\pi} \frac{\partial}{\partial \xi} H - \frac{\omega_c(\xi)}{\Omega_0} \frac{\partial}{\partial T} u, \\ \frac{\partial}{\partial T} u &= -\frac{1}{\tilde{T}_2 \omega_0} u - v, \\ \frac{\partial}{\partial T} v &= -\frac{1}{\tilde{T}_2 \omega_0} v + u + \frac{2\Omega_0}{\omega_0} E w, \\ \frac{\partial}{\partial T} w &= -\frac{1}{\tilde{T}_1 \omega_0} (w + 1) - \frac{2\Omega_0}{\omega_0} E v. \end{aligned} \quad (1)$$

Here,  $E = E_x/E_0$  and  $H = \sqrt{\mu_0/\epsilon_0} H_y/E_0$  are the normalized dimensionless components of the few-cycle pulse ( $E_0$  corresponds to the peak amplitude of the electric component of the incident pulse).  $\Omega_0 = gE_0/\hbar$  with the dipole moment  $g$  is the peak Rabi frequency of the incident pulse.  $\tilde{T}_1$  and  $\tilde{T}_2$  are, respectively, the lifetime of the excited state and the dephasing time. In the above equations, we have assumed that the transition frequency of the two-level atom is equal to the carrier frequency  $\omega_0$  of the pulse. Further,  $\omega_c(\xi) = N(\xi)g^2/\epsilon_0\hbar$  with  $N(\xi)$  denoting the density distribution of the atomic medium and which is given by the expression

$$\omega_c(\xi) = \begin{cases} d \text{ fs}^{-1} & \text{if } \xi \in [2n\delta, 2n\delta + \delta), \\ 0 & \text{if } \xi \in [2n\delta + \delta, 2n\delta + 2\delta), \end{cases} \quad (2)$$

where  $d$  and  $\delta$  express the atom density and the thickness of one layer.  $n$  is an integer between  $[0, L/(2\delta) - 1]$ . The density distribution of the atomic medium is shown in

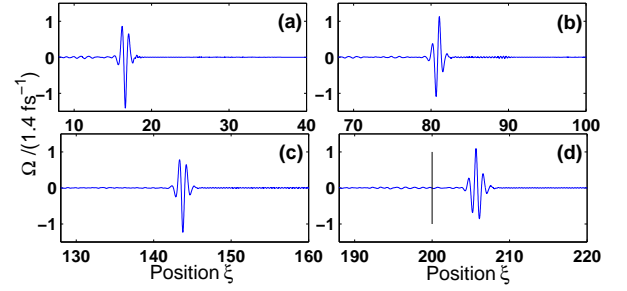


FIG. 2: (color online) Electric field profiles for different time moments. (a)  $t = 0.1$  ps; (b)  $t = 0.3$  ps; (c)  $t = 0.5$  ps; (d)  $t = 0.7$  ps. The other atomic and structure parameters are:  $\Omega_0 = 1.4 \text{ fs}^{-1}$ ,  $d = 0.2$ ,  $\delta = 0.25$  and  $\xi \in [0, 200]$ . (a) and (d) correspond to the electric field profiles near the input face and outside the exit face (vertical line in d), respectively.

Fig. 1. The incident pulse we consider is a few-cycle pulse with a hyperbolic secant envelope, i.e.,  $\Omega(T = 0, \xi) = \Omega_0 \cos[2\pi(\xi - \xi_0)] \text{sech}[1.76 \times 2\pi(\xi - \xi_0)/\tau_p]$ , where  $\tau_p$  is the full width half maximum (FWHM) of the pulse intensity envelope (see the red curve in Fig. 1). The choice of  $\xi_0$  ensures that the pulse locates in the free space and the partial pulse in the structure can be neglected at  $t = 0$ . The two-level medium is initialized with  $u = v = 0$  and  $w = -1$  at  $t = 0$ . The material and laser parameters are chosen as follows:  $\tau_p = 5 \text{ fs}$ ,  $\omega_0 = 2.3 \text{ fs}^{-1}$  ( $\lambda_0 = 830 \text{ nm}$ ),  $g = 2 \times 10^{-29} \text{ A s m}$ ,  $\tilde{T}_1 = 1 \text{ ps}$ ,  $\tilde{T}_2 = 0.5 \text{ ps}$ , and  $N = 4.4 \times 10^{20} \text{ cm}^{-3}$ . The above parameters give an atomic density  $d = 0.2$ . The peak Rabi frequency  $\Omega_0 = 1.4 \text{ fs}^{-1}$  corresponds to an input envelope area  $A = \Omega_0 \tau_p \pi / 1.76 = 4\pi$ . The cycle number of the initial pulse is about 1.83.

We have obtained numerical results of Eqs. (1) for different periodic structures. Firstly, let us investigate the few-cycle pulse propagation in a resonant structure in which the structure period  $2\delta$  exactly satisfies the Bragg condition:  $2\delta = m/2$  (the dimensionless coordinate is taken and  $m$  is an integer here). In our case, the period of the structure is set to be equal to  $1/2$ . The electric field profiles of the penetrating pulse inside and outside the periodic structure for different time moments are shown in Fig. 2. As can be observed, the pulse can maintain the same envelope to propagate which is a typical behavior of the gap solitons in periodic structures. Remarkably, the cycle number of the transmitted pulse is reduced in comparison to the initial pulse. We obtain a 0.85 cycle for the output pulse in Fig. 2(d). To further describe the system, we plot in Fig. 3 the inversion as well as the electric field profile at particular time-space coordinates. The distribution of inversion  $w$  is not continuous and in certain layers one can create population inversion. Therefore, the sideband parts of the propagating pulse annihilate while the central part slightly amplifies. Evidently, the output pulse energy is not increased in comparison to that of the initial applied pulse.

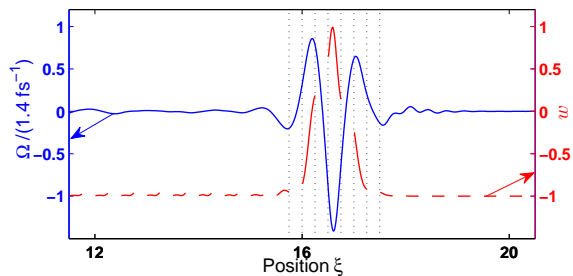


FIG. 3: (color online) Inversion population distribution (red curve) and electric field profile (blue curve) at time  $t = 0.1\text{ps}$ .  $\Omega_0 = 1.4 \text{ fs}^{-1}$ ,  $\delta = 0.25$ ,  $d = 0.2$  and  $\xi \in [0, 108]$ .

Subsequently, in order to clarify the soliton propagation in detail, we present in Fig. 4 the evolution of the pulse spectrum during propagation through a periodic structure when  $\delta = 0.25$ . Inspecting Fig. 4, we observe that the reflected and the penetrating spectra are situated around the input central frequency  $\omega_0$  which is distinct from the results of few-cycle propagation in the continuous media [8]. There, for  $d = 0.2$  and  $\xi = 108$ , the carrier frequency of the output pulse locates at  $1.16\omega_0$ . In our case, however, the large frequency shift of the transmitted and reflected pulses caused by intrapulse four-wave mixing can be efficiently suppressed. Periodic structures can usually offer optical band gaps similar to the flow of electrons in semiconductors and modulate the transmission of waves with different frequencies. In the same way, the periodic structure in our model is able to modify the dispersion property of the two-level atomic medium and destroy the phase-matching condition of four-wave mixing process which guarantees that the deformation of the penetrating pulse does not happen in our model. From here, we can conjecture that the periodic structure provides an alternative method for accurately preparing few-cycle pulses which will allow one to approach the experimental study of single-cycle optics [9]. Thus, we have demonstrated that single sub-cycle gap solitons can be formed in a periodic structure.

In the following, we will discuss the case of a few-cycle

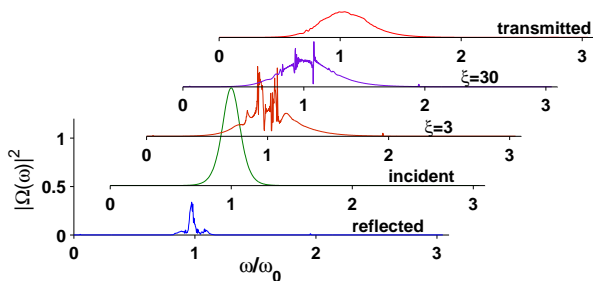


FIG. 4: (color online) Evolution of the pulse spectrum during propagation inside and outside the periodic structure. The atomic and structure parameters are the same as in Fig. (3).

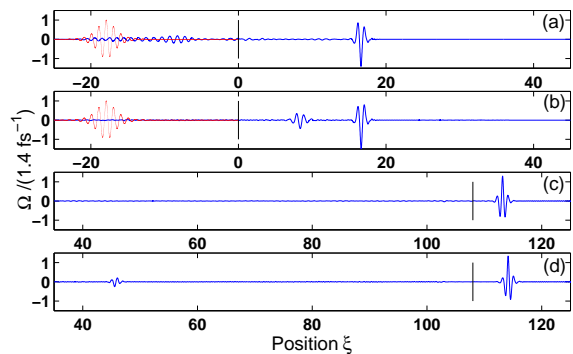


FIG. 5: (color online) Electric field profiles for different time moments and structure periods near the input face [(a),(b)] and outside the exit face [(c),(d)]. (a)  $t = 0.1\text{ps}$ ,  $\delta = 0.25$ ; (b)  $t = 0.1\text{ps}$ ,  $\delta = 0.1$ ; (c)  $t = 0.4\text{ps}$ ,  $\delta = 0.25$ ; (d)  $t = 0.4\text{ps}$ ,  $\delta = 0.1$ . Red line on the left of (a) and (b): incident pulse at  $t = 0$ . Here  $\Omega_0 = 1.4 \text{ fs}^{-1}$ ,  $d = 0.2$  and  $\xi \in [0, 108]$ .

pulse propagation in a tighter periodic structure which violates the Bragg condition. As a comparison, in Fig. 5, the initial, reflected, penetrating and transmitted pulses near the input face and outside the exit face are shown for different structure periods. In the simulation, the parameters are the same except for the structure period  $2\delta$ . For the case of tighter periodic structure ( $\delta = 0.1$ ), the penetrating part is strong enough to split into two pulses where the stronger of which moves faster than the weaker one that is unstable and decays quickly (see Fig. 5b and Fig. 5d). More energy of the incident pulse is located in the structure in this situation which is different from the case of  $\delta = 0.25$  (compare Fig. 5a with Fig. 5b). At the same time, by comparing with the profiles of the penetrating and transmitted pulses, one can observe that the incident pulse is dramatically shortened. We obtain the cycle number,  $N_c$ , for the FWHM of the intensity of the output pulse in Fig. 5(c,d) as  $N_c \simeq 1.76\tau/(2\pi)$  with  $\tau \approx 2.5$ . Thus, the cycle number  $N_c$  is about 0.7 which indicates that the gap soliton with less than one optical cycle can be formed in a subwavelength structure. The pulse propagation for other cases (i.e. for longer pulses and structure periods, slightly different and random layer widths, etc.) has been simulated, too, and the behavior of the penetrating pulse is similar to the situations shown in Fig. 2 - Fig. 5, though for longer pulses one can obtain fewer output stable pulses. If the atomic density is increased, the single-cycle gap soliton cannot be obtained for larger structures. The reason for this is that the reflection on the interfaces of the atomic layers is enhanced rapidly with the increase in the atomic density. The output field spreads and becomes weak. Similar things can happen if one moderately increases the initial pulse intensity. However, shorter structures ( $\xi \sim 20$ ) can lead to an output single-cycle pulse, too. If  $0.2 < d < 1$ , its carrier frequency slightly shifts towards higher frequencies when  $\Omega_0$  approaches  $\omega_0$  (the shift is smaller than that in

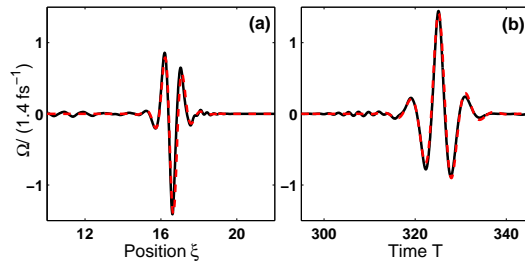


FIG. 6: (color online) Electric field profiles and corresponding fitting curves in space and time coordinates (a) for  $t = 0.1\text{ps}$ ; (b) for  $\xi = 30$ . The black and red lines represent the numerical result and the analytic solution  $\Omega^+$  given in Eq. (3), respectively.  $\Omega_0 = 1.4 \text{ fs}^{-1}$ ,  $\delta = 0.25$ ,  $d = 0.2$  and  $\xi \in [0, 200]$ .

a continuous sample with identical parameters).

In general, gap solitons are generated as a result of interaction of counterpropagation waves. As remarked above, the existence of gap soliton solution of the envelope equations is restricted by the validity of SVEA and RWA which is violated for the conditions considered here. However, in the above two approximations, the pulse propagation in a resonant periodic structure can be described by a set of semiclassical coupled-mode Maxwell-Bloch equations. Then, assuming that the pulse consists of two strong coupled modes that propagate in the structure, one can obtain a *sech*-form soliton solution which has the following form [17]:  $E^\pm = \hbar\Omega^\pm/g$ , where

$$\Omega^\pm = \Omega_m^\pm \text{sech}[(2\pi\xi - v_g T)/(v_g \tau)] \cos(2\pi\xi \mp T + \phi). \quad (3)$$

Here,  $E^+$  and  $E^-$  denote the electric-field amplitudes of the forward and backward waves.  $v_g$  and  $\tau$  are group velocity and pulse duration, respectively.  $\phi$  is an arbitrary phase factor while  $\Omega_m^\pm = \omega_0(1 \pm 1/v_g)/\tau$ . The relationship of parameters  $v_g$  and  $\tau$  is  $v_g^{-2} = 1 + 2\omega_c \tau^2 S/\omega_0$  with  $S$  depending on the broadened line form [17]. With the help of these results, one obtains the envelope areas of the forward and backward waves:  $A^\pm = \int \frac{\omega_0}{\tau} (1 \pm v_g^{-1}) \text{sech}[(2\pi\xi - v_g T)/(v_g \tau)] dt = \pi(1 \pm v_g^{-1})$  which is referred to as gap  $2\pi$  soliton [16, 17]. If the field amplitude is strong enough, the cycle number of the stable soliton will be small or less than one.

As an example, in Fig. 6, the electric field profiles and corresponding fitting curves in space and time coordinates are illustrated. Here, the group velocity  $v_g = (\xi_2 - \xi_1)/(t_2 - t_1) \approx 0.85$  where  $\xi_2$  and  $\xi_1$  are the positions of the pulse maxima at  $t_2$  and  $t_1$ , respectively, (see, for example, Fig. 2(a,c) whereas velocity unit is the light velocity in vacuum). The pulse duration is  $\tau \approx 2.5$ . Due to the fact that the pulse curves are mainly determined by the forward wave in the early stage of the formation of gap soliton, the fitting function is taken to be of the form of a forward wave  $\Omega^+$ , i.e.,  $\Omega^+ = (\omega_0/\tau)(1 + 1/v_g) \text{sech}[2\pi(\xi - \xi_m)/(v_g \tau)] \cos(2\pi(\xi - \xi_m) + \phi_\xi)$  when  $t$  is fixed while  $\Omega^+ = (\omega_0/\tau)(1 + 1/v_g) \text{sech}[-(T -$

$T_m)/\tau] \cos(-(T - T_m) + \phi_T)$  when  $\xi$  is fixed.  $\{\xi_m, T_m\}$  and  $\{\phi_\xi, \phi_T\}$  describe the corresponding positions of the maxima of the profile pulse given by Eqs. (1). In particular, we obtain  $\xi_m \approx 16.6$ ,  $T_m \approx 325.5$ ,  $\phi_\xi \approx 0.87\pi$  and  $\phi_T \approx 1.9\pi$  for the curves shown in Fig. 6. Here, one interesting result is that the *sech*-form solution derived from the semiclassical coupled-mode Maxwell-Bloch equations within the frame of SVEA and RWA coincides well with the numerical results in our model. With the further evolution of the penetrating pulse, the electric field profiles will depend on the forward and backward waves.

In summary, we demonstrated the formation of a single sub-cycle gap soliton when a few-cycle laser pulse penetrates a subwavelength structure. The carrier frequency of the output pulse is located around the frequency of the initial laser pulse. The proposed scheme works even for the case of broken Bragg condition as well as slightly different random layer widths. The corresponding analytical solution of the single-cycle gap soliton was given.

We acknowledge helpful discussions with Christoph H. Keitel and Karen Z. Hatsagortsyan.

\* Electronic address: xtxie@nwu.edu.cn

† Electronic address: mihai.macovei@mpi-hd.mpg.de

- [1] T. Brabec, F. Krausz, Rev. Mod. Phys. **72**, 545 (2000); T. Udem, R. Holzwarth, T. W. Hänsch, Nature **416**, 233 (2002).
- [2] V. V. Lozovoy, M. Dantus, Annu. Rep. Prog. Chem. C **102**, 227 (2006).
- [3] A. H. Zewail, J. Phys. Chem. A **104**, 5660 (2000).
- [4] C. J. Bardeen et al., J. Biomed. Opt. **4**, 362 (1999).
- [5] D. Goswami, Phys. Rep. **374**, 385 (2003).
- [6] H. Leblond, Phys. Rev. A **78**, 013807 (2008); H. Leblond, I. V. Mel'nikov, D. Mihalache, *ibid* **78**, 043802 (2008).
- [7] S. A. Skobelev, D. V. Kartashov, A. V. Kim, Phys. Rev. Lett. **99**, 203902 (2007).
- [8] V. P. Kalosha, J. Herrmann, Phys. Rev. Lett. **83**, 544 (1999).
- [9] T. Brabec and F. Krausz, Phys. Rev. Lett. **78**, 3282 (1997); E. Goulielmakis et al, Science **320**, 1614 (2008).
- [10] G. Steinmeyer et al., Science **286**, 1507 (1999); M. Wegener, *Extreme Nonlinear Optics: An Introduction* (Springer, Berlin 2005).
- [11] J. E. Rothenberg, Opt. Lett. **17**, 1340 (1992); Yueping Niu et al., Phys. Rev. A **78**, 063835 (2008).
- [12] K. Busch et al., Phys. Rep. **444**, 101 (2007).
- [13] M. Scalora et al., Phys. Rev. Lett. **73**, 1368 (1994).
- [14] B. J. Eggleton et al., Phys. Rev. Lett. **76**, 1627 (1996).
- [15] G. Kurizki et al., in *Progress in Optics*, edited by E. Wolf (Elsevier, North-Holland, 2001), Vol. 42, p. 93.
- [16] A. Kozhokin, G. Kurizki, Phys. Rev. Lett. **74**, 5020 (1995).
- [17] B. I. Mantsyzov, Phys. Rev. A **51**, 4939 (1995).
- [18] G. S. Agarwal, T. Dey, Phys. Rev. A **75**, 043806 (2007).
- [19] G. Khitrova et al., Rev. Mod. Phys. **71**, 1591 (1999).
- [20] R. W. Ziolkowski, J. M. Arnold, D. M. Gogny, Phys. Rev. A **52**, 3082 (1995).